Structure of Conduction Electrons on Polysilanes As Studied by Electron Spin-Echo Envelope Modulation Analysis

Tsuneki Ichikawa,* Hitoshi Koizumi, and Jun Kumagai

Division of Molecular Chemistry, Graduate School of Engineering, Hokkaido University, Sapporo 060, Japan

Received: June 25, 1997; In Final Form: October 7, 1997[⊗]

The orbital structures of conduction electrons on permethylated oligosilane, $Si_8(CH_3)_{18}$, and poly(cyclohexylmethylsilane) have been determined by analyzing the electron spin-echo envelope modulation signals of the radical anions of these silanes in a deuterated rigid matrix at 77 K. The conduction electron on permethylated oligosilane is delocalized over the entire main chain, whereas that on poly(cyclohexylmethylsilane) is localized on a part of the main chain composed of about six Si atoms. Quantum-chemical calculations suggest that Anderson localization due to fluctuation of σ conjugation by conformational disorder of the main chain is responsible for the localization of both the conduction electron and the hole.

Introduction

Polysilanes are σ-conjugated polymers composed of Si−Si skeletons and organic side chains. Although polysilanes are insulators with bandgaps of ca. 4 eV,[1,2] they can be converted to one-dimensional conductors either by photoexcitation or by doping electron donors or acceptors. The electric conductivity of polysilanes depends on the degree of delocalization of charge carriers, electrons in the conduction band, and/or holes in the valence band, over the polymer chain. High electric conductivity cannot be expected if the charge carriers are localized on a small part of the polymer chain. To elucidate the structure of the charge carriers is therefore important for the development of polysilanes as one-dimensional conducting polymers.

The structures of the charge carriers have been studied by analyzing the electronic absorption spectra and the ESR spectra of the radical anion and cation of polysilanes[3−12] possessing an excess electron and a hole in the conduction and the valence bands of the silicon main chain, respectively. Of these spectroscopic methods, ESR is especially useful, since it gives the direct information on the structure of ground-state charge carriers through hyperfine interactions between the electron spins of the charge carriers and the nuclear spins of the pendant groups. By analyzing hyperfine interactions, we have found that the hole in the radical cation of permethylated oligosilanes is delocalized over the entire main chain, whereas that of polysilanes, poly(cyclohexylmethylsilane) and poly(methylphenylsilane) is localized on a part of the chain composed of six Si atoms.[11] We have also found that the hole in the radical cations is delocalized onto the pendant groups, whereas the conduction electron in the radical anions is confined within the silicon main chain.[12] This observation suggests that the pendant groups hinder the interchain hopping of conduction electrons but not holes. Although analysis of the ESR *g* anisotropy and the optical absorption spectra suggested that the conduction electron on polysilanes is also localized on a part of the main chain,[10] because of very weak hyperfine interactions, the detailed structure of the conduction electron has not been determined yet.

In the present paper the ESEEM (electron spin-echo envelope modulation) signals for the radical anions of permethylated oligosilane and poly(cyclohexylmethylsilane) arising from hyperfine interactions between unpaired electrons and deuterons of surrounding solvent have been analyzed for determining the detailed structure of the conduction electrons on the silicon main chains.

Experimental Section

Permethylated oligosilanes, $Si_n(CH_3)_{2n+2}$, where n is 6 and 8, were synthesized from $Si_{n/2}(CH_3)_{n+1}Cl$ by Wurtz-type reaction[10] and purified by fractional distillation. Poly(cyclohexylmethylsilane), $(-SiCH_3C_6H_{11}-)_n$, was synthesized from dichlorocyclohexylmethylsilane by Wurtz type reaction in the mixed solvent of toluene and *n*-heptane (0.85:0.15) with Na−K alloy and 15-crown-5 ether under the reflux condition.[13] The crude polymer was purified by repeated precipitation from the chloroform solution into methanol. The gel permeation chromatographic measurement showed that the average number of Si atoms composing the polymer main chains was approximately 500. The number of $-Si(Si-)_2-$ branches per a main chain was estimated from the ^{29}Si NMR spectrum to be less than 0.7.

Perdeuterated methylcyclohexane (98% D) containing 5 vol % of perdeuterated tetrahydrofuran as a hole scavenger was used as a solvent for electron spin-echo measurements. Nuclear modulation effect giving the information on the spatial distribution of unpaired electrons on polysilanes was detected more easily for deuterated solvents. The solvent was vacuum-distilled with Na−K alloy as a drying agent and then deaerated by freeze−pump−thaw cycles. About 0.01 mol/dm^3 of $Si_n(CH_3)_{2n+2}$ or $(-SiCH_3C_6H_{11}-)_n$ (monomer unit) was dissolved under vacuum in the solvent in a high-purity quartz tube. The solution in the vacuum-sealed tube was frozen at 77 K and then irradiated in the dark with a ^{60}Co γ-ray source to a dose of 100 kGy. The radiation-chemical process induced by γ-irradiation is

$$MCHX + \gamma \rightarrow MCHX^+ + e^-,$$

$$MCHX^+ + THF \rightarrow MCHX^\bullet + THFH^+$$

$$e^- \rightarrow e_t^-, \quad e^- + Si_n \rightarrow Si_n^-$$

where MCHX and MCHX$^\bullet$ are methylcyclohexane and its radical generated by proton detachment, THF and $THFH^+$ are tetrahydrofuran and protonated one, e_t^- is a trapped electron, and Si_n is a solute molecule. Since the absorption of radiation energy is a statistical process, direct radiation damage is negligible for solute molecules with low concentration. Elec-

[⊗] Abstract published in *Advance ACS Abstracts,* December 1, 1997.

S1089-5647(97)02068-3 CCC: $14.00

trons ejected mainly from MCHX by γ-rays were captured by solute molecules to generate solute radical anions. Coexisting trapped electrons in the irradiated samples were eliminated before the measurements by photoillumination of the samples with near-IR light of the wavelength longer than 800 nm. The temperature of the samples was kept at 77 K throughout the experiments.

The electron spin-echo (ESE) signals were measured with a homemade ESE spectrometer[14] by using $\pi/2-\pi$ two pulse sequences. The ESE-detected ESR spectra were measured by recording the intensity of the ESE signals while sweeping the magnetic field very slowly.

Data Analysis

The relative configuration of deuterons with respect to an unpaired electron, or *vice versa*, can be obtained by comparing the observed ESEEM with theoretical ones under assumed configurations. The two-pulse ESEEM signal arising from magnetic interaction between an unpaired electron located at **r** and a nucleus located at **R** is given by a third-order perturbation method as[15,16]

$$\begin{aligned}\epsilon(r,R,\xi,\tau) = 1 - [\omega_I B/(\omega_\alpha\omega_\beta)]^2\{I(I+1)/3\}[\cos(\omega_\alpha\tau - \omega_\beta\tau)C_1(\gamma_\alpha\tau - \gamma_\beta\tau) + \cos(\omega_\alpha\tau + \omega_\beta\tau)C_1(\gamma_\alpha\tau + \gamma_\beta\tau) - 2\cos(\omega_\alpha\tau)C_1(\gamma_\alpha\tau) - 2\cos(\omega_\beta\tau)C_1(\gamma_\beta\tau) + 2] + [\omega_I B/(\omega_\alpha\omega_\beta)]^3 B(B\gamma + 2A\mu_1 - B\mu_2)[2\sin(\omega_\alpha\tau)S_1(\gamma_\alpha\tau) + 2\sin(\omega_\beta\tau)S_1(\gamma_\beta\tau) - \sin(\omega_\alpha\tau + \omega_\beta\tau)S_1(\gamma_\alpha\tau + \gamma_\beta\tau) + \sin(\omega_\alpha\tau - \omega_\beta\tau)S_1(\gamma_\alpha\tau - \gamma_\beta\tau)] + [\omega_I B/(\omega_\alpha\omega_\beta)]^4\{I(I+1) \times (2I-1)(2I+3)/240\}[12\cos(\omega_\alpha\tau - \omega_\beta\tau)C_2(\gamma_\alpha\tau - \gamma_\beta\tau) + 12\cos(\omega_\alpha\tau + \omega_\beta\tau)C_2(\gamma_\alpha\tau + \gamma_\beta\tau) - 24\cos(\omega_\alpha\tau)C_2(\gamma_\alpha\tau) - 24\cos(\omega_\beta\tau)C_2(\gamma_\beta\tau) + \cos(2\omega_\alpha\tau - 2\omega_\beta\tau)C_3(4\gamma_\alpha\tau - 4\gamma_\beta\tau) + \cos(2\omega_\alpha\tau + 2\omega_\beta\tau)C_3(4\gamma_\alpha\tau + 4\gamma_\beta\tau) + 6\cos(2\omega_\alpha\tau)C_3(4\gamma_\alpha\tau) + 6\cos(2\omega_\beta\tau)C_3(4\gamma_\beta\tau) + 4\cos(\omega_\alpha\tau - \omega_\beta\tau)\cos(\gamma_\alpha\tau + \gamma_\beta\tau)C_3(2\gamma_\alpha\tau - 2\gamma_\beta\tau) + 4\cos(\omega_\alpha\tau + \omega_\beta\tau)\cos(\gamma_\alpha\tau - \gamma_\beta\tau)C_3(2\gamma_\alpha\tau + 2\gamma_\beta\tau) - 4\cos(2\omega_\alpha\tau + \omega_\beta\tau)\cos(\gamma_\beta\tau)C_3(4\gamma_\alpha\tau + 2\gamma_\beta\tau) - 4\cos(2\omega_\alpha\tau - \omega_\beta\tau)\cos(\gamma_\beta\tau)C_3(4\gamma_\alpha\tau - 2\gamma_\beta\tau) - 4\cos(\omega_\alpha\tau + 2\omega_\beta\tau)\cos(\gamma_\alpha\tau)C_3(2\gamma_\alpha\tau + 4\gamma_\beta\tau) - 4\cos(\omega_\alpha\tau - 2\omega_\beta\tau)\cos(\gamma_\alpha\tau)C_3(2\gamma_\alpha\tau - 4\gamma_\beta\tau) + 18] \quad (1)\end{aligned}$$

where τ is a time interval between the first and the second microwave pulses and also between the second pulse and the time of ESE observation

$$A = [1/(\hbar|\mathbf{r} - \mathbf{R}|^3)]gg_N\beta\beta_N(3\cos^2\theta - 1) + 2\pi a$$

$$B = [3/(\hbar|\mathbf{r} - \mathbf{R}|^3)]gg_N\beta\beta_N\sin\theta\cos\theta$$

$$\omega_I = g_N\beta_N H/\hbar, \quad \gamma' = \{3e^2qQ/[8I(2I-1)\hbar]\}$$

$$\gamma = \gamma'(3\cos^2\theta' - 1), \quad \omega_{\alpha,\beta} = [(\omega_I \mp A/2)^2 + B^2/4]^{1/2}$$

$$\gamma_{\alpha,\beta} = \gamma'\{3[(\omega_I \mp A/2)\cos\theta \mp (B/2)\sin\theta\cos(\phi - \phi')]/\omega_{\alpha,\beta}{}^2 - 1\}$$

$$\mu_1 = \gamma'\sin\theta'\cos\theta'\cos(\phi' - \phi),$$

$$\mu_2 = (\gamma'/2)\sin^2\theta'\cos(2\phi' - 2\phi)$$

$$C_1(x) = \{3/[2I(I+1)(2I+1)]\}\sum_{m=-I}^{I}\{I(I+1) - m(m+1)\}\cos\{(2m+1)x\}$$

$$S_1(x) = [1/(2I+1)]\sum_{m=-I}^{I}\{I(I+1) - m(m+1)\}(2m+1)\sin\{(2m+1)x\}$$

$$C_2(x) = \{15/[2I(I+1)(2I-1)(2I+1)(2I+3)]\} \times \sum_{m=-I}^{I}\{I(I+1) - m(m+1)\}\{I(I+1) - (m^2+m+1)\} \times \cos\{(2m+1)x\}$$

$$C_3(x) = \{15/[2I(I+1)(2I-1)(2I+1)(2I+3)]\} \times \sum_{m=-I}^{I}\{I(I+1) - m(m+1)\}\{I(I+1) - m(m-1)\}\cos(mx)$$

θ and ϕ are the polar and azimuthal angles of vector $r - R$ joining the unpaired electron and the nucleus with nuclear spin I, isotropic hyperfine coupling constant a, and quadrupole frequency e^2qQ/h with respect to z as a polar axis parallel to the external magnetic field H, and θ' and ϕ' are the polar and azimuthal angles of unit vector ξ indicating the direction of the quadrupole moment with respect to z. The location of an unpaired electron in a paramagnetic center is not uniquely determined but is expressed by a wave function $\psi(\sigma,\mathbf{r})$, where σ is a unit vector indicating the direction of the molecular axis of the paramagnetic center. The ESEEM signal is then given by

$$E(\sigma,R,\xi,\tau) = \int\psi^*(\sigma,r)\,\psi(\sigma,r)\,\epsilon(r,R,\xi,\tau)\,d^3r \quad (2)$$

For an unpaired electron interacting with M nuclei, the observed ESEEM signal is given by

$$V(\tau) = D(\tau)\int\int\int\ldots\int[P(\sigma,R_1,\ldots,R_M,\xi_1,\ldots,\xi_M)\prod_{j=1}^{M} \times E(\sigma,R_j,\xi_j,\tau)]\,d^2\xi_1\,d^2\xi_2\ldots d^2\xi_M\,d^2\sigma \quad (3)$$

where $D(\tau)$ is a monotonous decay function of the phase relaxation, $P(\sigma,R_1,\cdots R_M,\xi_1,\cdots x_M)$ is the probability that ESE intensity of the paramagnetic center with molecular and nuclear configurations σ, $R_1,\cdots R_M$, ξ_1, $\cdots$, x_M, and the electronic configuration $\psi(\sigma,r)$ is detected by an electron spin-echo spectrometer. For relatively shallow ESEEM signals, a ratio analysis method is applicable for eliminating $D(\tau)$ from the observed signal.[17] In this method, the data analysis proceeds by drawing curves through the maxima and minima of the ω_I component of the modulation pattern. Then the experimental ratio of these two curves, V_{min}/V_{max}, is determined as a function of τ.

Calculation of the ESEEM signal requires the knowledge about the wave function of an unpaired electron in a paramagnetic molecule and the orientation of deuterons with respect to the paramagnetic molecule. We used the following approximations for oligosilane and polysilane radical anions;

1. The molecular structures of the radical anions are the same as those of the precursor molecules, since the molecular structures cannot be changed much in the rigid cryogenic matrix.

2. Polysilanes are composed of Si−Si skeletons surrounded by nondeuterated organic pendant groups, and the excess electrons are confined on the Si−Si chains. The structure of these silane radical anions is therefore approximated by a rod with a linear silicon wire embedded at the center of the rod composed of nondeuterated organic pendant groups. Using the Si−Si bond length of 0.235 nm and the Si−Si−Si bond angle of 115.4°,[18,19] the length of the wire per one Si−Si bond is estimated to be 0.199 nm.

3. An unpaired electron is shared by N Si atoms composing a part of the central wire. We have shown in a previous paper[10] that the atomic orbitals for an unpaired electron on polysilane are 3p orbitals of the Si atoms. The molecular orbital for the unpaired electron is therefore similar to that of the lowest orbital of a π-conjugated polyene. Using a simple Huckel approximation, the orbital is given as

$$\psi(\sigma,\mathrm{r}) = \sqrt{\frac{2}{N+1}}\sum_{n=1}^{N}\sin\left(\frac{n\pi}{N+1}\right)\phi_n(r_n - r) \qquad (4)$$

where $\phi_n(r_n - r)$ is the 3p atomic orbital of the n-th silicon atom located at r_n in the wire with the molecular axis σ. Since the frequency of the electron motion is much faster than the ESR frequencies, the ESEEM signal of the radical anion interacting with one nucleus is given by averaging out a magnetic dipolar interaction between the fixed nucleus and the delocalized unpaired electron all over the possible locations of the electron, as

$$E(\sigma,R,\xi,\tau) = \int \psi^*(\sigma,r)\,\psi(\sigma,r)\,\epsilon(r,R,\xi,\tau)\,\mathrm{d}^3r$$

$$= \int\left[\sqrt{\frac{2}{N+1}}\sum_{n=1}^{N}\sin\left(\frac{n\pi}{N+1}\right)\phi_n(r_n - r)\right]^2 \epsilon(r,R,\xi,\tau)\,\mathrm{d}^3r$$

$$\approx \frac{2}{N+1}\sum_{n=1}^{N}\sin^2\left(\frac{n\pi}{N+1}\right)\epsilon(r_n,R,\xi,\tau) \qquad (2')$$

In the above equation the atomic orbitals are approximated by Dirac δ functions. In other words, the average location of the unpaired electron in an atomic orbital is assumed to be the center of the orbital. It can be deduced from eq 2′ that the ESEEM cannot be expected for an unpaired electron delocalized all over the main chain of polysilane with $N \approx \infty$, since the average distance between the electron and a nucleus becomes infinite.

4. $P(\sigma,\mathrm{R}_1,...R_M,\xi_1,...,x_M)$ is the same for all the radical anions, since more than 70% of the radical anions are excited and detected by microwave pulses used in the present measurements.

5. Deuterons are homogeneously distributed around an anion and the direction of the quadrupole moments of the deuterons are random, since no specific solute−solvent interaction is expected between the radical anions and the nonpolar solvent.

Simplifications 4 and 5 allows us to eliminate integration over all possible locations of nuclei and the directions of their quarupole moments. For weak quadrupole interactions it is possible to express

$$V(\tau) = D(\tau)\int\int\int...\int[P(\sigma,R_1,\ ...\ R_M,\xi_1,\ ...\ \xi_M)\times \prod_{j=1}^{M}E(\sigma,R_j,\xi_j,\tau)]\,\mathrm{d}^2\xi_1\,\mathrm{d}^2\xi_2\ ...\ \mathrm{d}^2\xi_M\,\mathrm{d}^2\sigma$$

$$\approx D((\tau)\int\prod_{j=1}^{M}E(\sigma,R_j,\xi_{j,\mathrm{rand}},\tau)]\,\mathrm{d}^2\sigma \qquad (3')$$

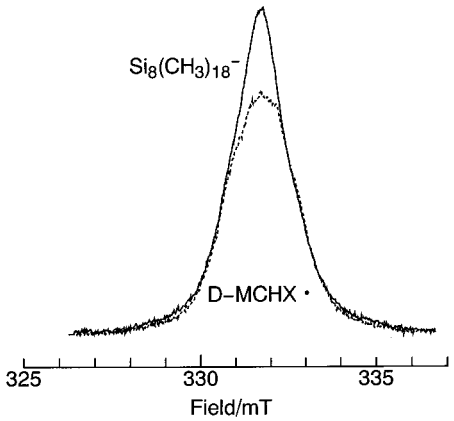

Figure 1. Two-pulse ESE-detected ESR spectra at 77 K for γ-irradiated perdeuterated methylcyclohexane containing 5 vol % of perdeuterated tetrahydrofuran and 0.01 mol/dm^3 of $Si_8(CH_3)_{18}$ before (solid line) and after (broken line) photobleaching the radical anion of $Si_8(CH_3)_{18}$. The time interval between the first and the second microwave pulses was fixed at 600 ns.

where R_j is the location of the j-th deuteron and $\xi_{j,\mathrm{rand}}$ is the direction of its quadrupole moment defined by a random variable. It is noted that only the averaging over the orientation of the anion, σ, with respect to the external field is necessary for the calculation of the ESEEM signal. The locations of deuterons were given as follows.

We first measured the specific gravity of each polysilane at 77 K (0.87 for all the polysilanes examined) and determined the molecular volume. The cross section of a rod corresponding to one polysilane molecule was then determined by dividing the molecular volume with the length of the rod which in turn was determined from the number of Si atoms composing the central wire. The cross section was assumed to be circular or elliptical for $Si_n(CH_3)_{2n+2}$ or $(-SiCH_3C_6H_{11}-)_n$, respectively. The solvent around the rod was then separated into solvation shells with the thickness close to 0.226 nm (the width of a cube of the solvent containing one deuteron). The number of deuterons in the j-th solvation shell, M_j, was equal to the volume of the shell divided by the volume per one deuteron, 0.0116 nm^3, which was estimated from the density and the purity of the solvent. Each solvation shell was further divided into cubelike blocks with the volume corresponding to one deuteron. The location of a deuteron in the k-th block of the j-th solvation shell, $R_{j,k}$, was assumed to be the center of the cubelike block. The ESEEM signal necessary for the calculation of $V_{\min}/V_{\max}$ was obtained by using

$$V(\tau) = \int\{\prod_{j=1}^{\infty}\prod_{k=1}^{M_j}E(\sigma,R_{j,k},\xi_{j,k,\mathrm{rand}},\tau)\}\,\mathrm{d}^2\sigma \qquad (3'')$$

Results

Figure 1 shows the two-pulse ESE-detected ESR spectrum of a γ-irradiated sample containing $Si_8(CH_3)_{18}$. The irradiated sample contains both the solvent radical and the solute radical anion as paramagnetic species, and their ESR spectra overlap each other. Although the intensity of the conventional ESR spectrum of the $Si_8(CH_3)_{18}$ radical anion is much stronger than that of the solvent radical, because of its very fast phase relaxation, the ESE signal is much weaker than that of the solvent radical. The ESE signal of the $Si_6(CH_3)_{14}$ radical anion was not observed because of its too fast phase relaxation. The $Si_8(CH_3)_{18}$ radical anion disappeared after illumination of the sample with visible light, so that the ESE signal of the radical anion was obtained as a difference of the ESE intensities before

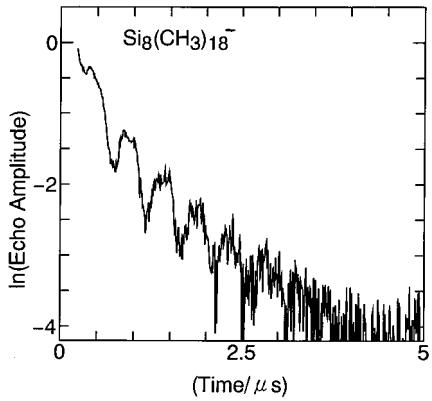

Figure 2. Two-pulse ESEEM signal of the $Si_8(CH_3)_{18}$ radical anion obtained by subtracting the contribution of the solvent radical on the observed ESE signal.

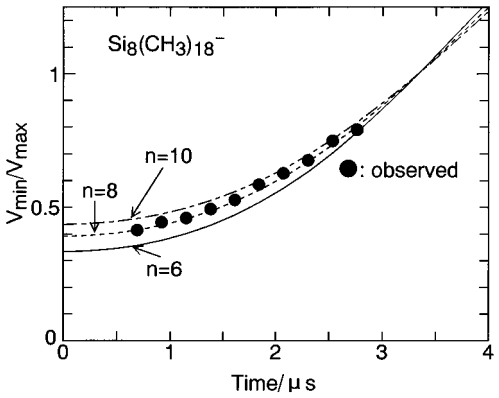

Figure 3. Comparison of the observed ESEEM signal of the $Si_8(CH_3)_{18}$ radical anion (●) and the simulated signals of $Si_n(CH_3)_{2n+2}$ radical anions (lines) in the mixed solvent of perdeuterated methylcyclohexane and 5 vol % perdeuterated tetrahydrofuran at 77 K. The ESEEM is expressed with the ratios of the observed or intrapolated modulation minima, V_{min}, to maxima, V_{max}. Simulations were carried out by simplifying the molecular structure of $Si_n(CH_3)_{2n+2}$ to be a cylinder of the radius 0.4 nm with a central linear wire corresponding to the Si−Si main chain. An unpaired electron is assumed to be delocalized on Si atoms composing the wire.

and after the photoillumination. Figure 2 shows the ESE signal of the radical anion thus obtained. The periodic modulation on the envelope signal, ESEEM, arises from magnetic interactions between the unpaired electron of the radical anion and the deuterons of perdeuterated solvent molecules. Nuclear modulation by protons of the pendant group is too weak to be observed on the envelope.

Figure 3 compares the observed and calculated ratios between the maxima and the minima of the two-pulse ESEEM signal as a function of the number of Si atoms composing $Si_n(CH_3)_{2n+2}$. The molecular shape of $Si_n(CH_3)_{2n+2}$ was assumed to be a cylinder. The diameter of the cylinder was estimated from the molecular volume of $Si_8(CH_3)_{18}$ (0.945 nm^3, estimated from the specific gravity of 0.87) to be 0.8 nm by assuming that the molecular shape of $Si_8(CH_3)_{18}$ was a cylinder terminated with two hemispheres with the diameter same as that of the cylinder. For simplifying the calculation, the length of a cylinder corresponding to the $Si_n(CH_3)_{2n+2}$ was then readjusted in such a way that the volume of the cylinder without the hemispheres was the same as the molecular volume of $Si_n(CH_3)_{2n+2}$. The diameter of the cylinder and the length of the central wire were unchanged. The best fit of the observed signal gives the number of Si atoms to be eight, which accords with the number of Si atoms composing the main chain. The ESEEM result supports our previous conclusion that the unpaired electron in the radical

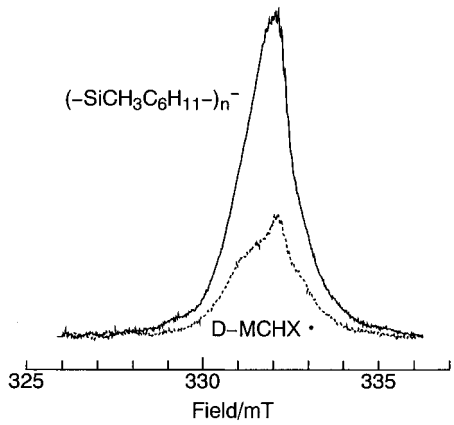

Figure 4. Two-pulse ESE-detected ESR spectra at 77 K for γ-irradiated perdeuterated methylcyclohexane containing 5 vol % of perdeuterated tetrahydrofuran and 0.01 mol/m^3 (monomer unit) of $(-SiCH_3C_6H_{11}-)_n$ before (solid line) and after (broken line) photobleaching the radical anion of $(-SiCH_3C_6H_{11}-)_n$. The time interval between the first and the second microwave pulses was fixed at 600 ns.

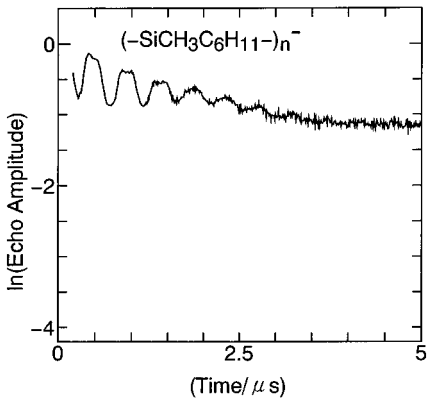

Figure 5. Two pulse ESEEM signal of the $(-SiCH_3C_6H_{11}-)_n$ radical anion obtained by subtracting the contribution of the solvent radical on the observed ESE signal.

anion of $Si_n(CH_3)_{2n+2}$ is delocalized over the entire Si skeleton.[10] Analysis of the ESEEM signal of the $(-SiCH_3C_6H_{11}-)_n$ radical anion is therefore expected to give a reliable result on the distribution of the conduction electron.

Figure 4 shows the ESE-detected ESR spectrum of a γ-irradiated sample containing $(-SiCH_3C_6H_{11}-)_n$. Although the yield of the $(-SiCH_3C_6H_{11}-)_n$ radical anion is not higher than that of the $Si_8(CH_3)_{18}$ radical anion, because of its slow phase relaxation (see Figure 5), the ESE intensity is much higher than that of the solvent radical. The phase relaxation rate of linear molecules in rigid solids generally increases with decreasing molecular length, since the molecular motion causing the fluctuation of magnetic interactions is much easier for shorter molecules.[20]

Figure 6 shows the ratio between the maxima and the minima of the two-pulse ESEEM signals of the $(-SiCH_3C_6H_{11}-)_n$ radical anion. Since the radical anion has methyl and cyclohexyl side chains, it is reasonable to assume that the radical anion has a rodlike structure with infinite length and with an elliptical cross section; the short and the long axes of the ellipsis correspond to the methyl and the cyclohexyl groups, respectively. Taking the short axis to be equal to the diameter for the $Si_8(CH_3)_{18}$ radical anion, 0.8 nm, the long axis is estimated from the area of the ellipsis, 1.32 nm^2, to be 2 nm. The best fit of the observed ESEEM is obtained by assuming that the unpaired electron is confined to a part of the main chain composed of only six Si atoms. It is evident that the unpaired conduction electron in the radical anion of $(-SiCH_3C_6H_{11}-)_n$

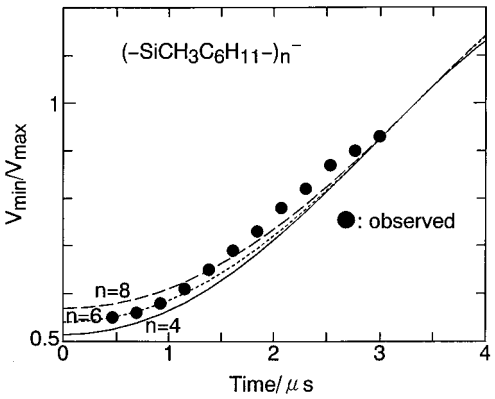

Figure 6. Comparison of the observed (●) and simulated (lines) ESEEM signals of the $(-SiCH_3C_6H_{11}-)_n$ radical anion in the mixed solvent of perdeuterated methylcyclohexane and 5 vol % perdeuterated tetrahydrofuran at 77 K. The amplitude of the ESEEM is expressed with V_{min}/V_{max}. Simulations were carried out by simplifying the structure of a polymer molecule to be a linear rod with an elliptic cross section and with a central wire corresponding to the Si−Si main chain. The short and the long axes of the ellipsis were 0.8 and 2.0 nm, respectively. An unpaired electron was assumed to be on a part of the wire composed of *n* Si atoms.

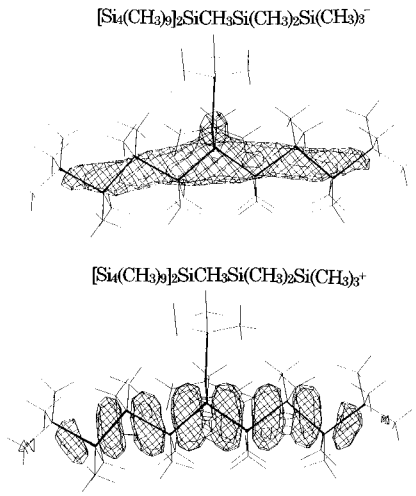

Figure 7. Distribution of unpaired electrons on the radical anion and cation of branched $[Si_4(CH_3)_9]_2Si(CH_3)_2Si(CH_3)_3$ obtained by semiempirical PM3 calculation. The hatched parts show the iso-surface of the spin density at 0.001.

(and probably (polyphenylmethylsilane)) is not delocalized over the entire Si main chain.

Discussion

The ESEEM result shows that the conduction electron in $(-SiCH_3C_6H_{11}-)_n$ is trapped on a part of the main chain. Localization of the electron apparently necessitates a structural irregularity on the main chain of the polymer. Two types of structural irregularities have been proposed as defects causing the localization of electrons on a part of the main chain. One is chemical defects induced by irregular chemical reactions during polymerization. Branching of the main chain has been suggested to be an important chemical defect for trapping an excited electron.[21] We have proposed that the branch also acts as a trap for the hole and the conduction electron.[10,11] However, this proposal should be discarded, because most of polymer molecules used in the present experiment do not have branches. Moreover, as shown in Figure 7, a quantum-chemical calculation (semiempirical PM3) indicates that a branch does not act as an efficient electron tap for a conduction electron and a hole.

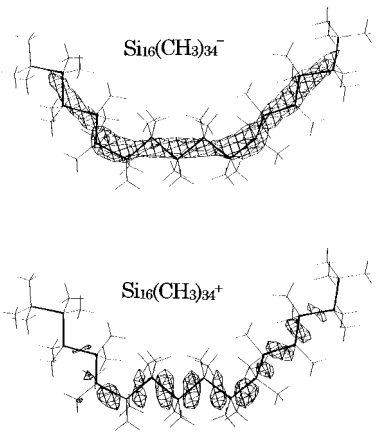

Figure 8. Distribution of unpaired electrons on the radical anion and cation of trans $Si_{16}(CH_3)_{34}$ with two cis conformations obtained by semiempirical PM3 calculation. The hatched parts show the iso-surface of the spin density at 0.001.

The other candidate is conformational defects which have been proposed for explaining the transfer and the inhomogeneous broadening of the excitation of polysilanes. Two models have been proposed for the structural defects. One is the chain segment model which assumes that a few defects distributed at random along a regular chain, such as cis (or gauche) Si−Si−Si conformation along a trans (or anti) linear chain, prevent the coherence of electrons and serves to localize excitations on mutually decoupled segments. The chain segment model has been applied successfully for explaining the photophysical and photochemical properties of polysilanes.[22−25]

The other model is the continuous disorder model which assumes a Gaussian distribution of σ-conjugation energies along the Si−Si main chain.[26−28] The Gaussian distribution arises from the irregular deformation of polymer backbone, so that this is also called the wormlike chain model. Localization of electronic states arises from the accumulation of energy mismatch between adjacent σ-conjugations, so that the localization is essentially Anderson localization.[29] This model was applied for explaining the electronic structure and energy transfer dynamics of poly(di-*n*-hexylsilane) in cryogenic solids and was concluded to be better than the chain segment model.

In the present study, localization of an unpaired electron on a part of the main chain was not observed for $Si_8(CH_3)_{18}$ with the main chain not long enough for the accumulation of the mismatch. This strongly suggests that the continuous disorder model or Anderson localization is applicable for the localization of the conduction electron on $(-SiCH_3C_6H_{11}-)_n$. Figure 8 shows the distribution of the unpaired electrons on the radical anion and cation of $Si_{16}(CH_3)_{34}$ obtained by the semiempirical PM3 calculation. The calculation shows that the introduction of trans−cis links in an otherwise all-trans main chain is not enough for inducing the localization of both the conduction electron and the hole, which also supports the validity of Anderson localization of both the conduction electron and the hole on silane polymers.

Acknowledgment. This work was supported by a grant-in-aid for Scientific Research from the Ministry of Education, Science and Culture, Japan.

References and Notes

(1) Takeda, K.; Shiraishi, K. *Phys. Rev. B* **1989,** *39,* 11028.
(2) Yokoyama, K.; Yokoyama, M. *Chem. Lett.* **1989,** 1005.
(3) Carberry, E.; West, R.; Glass, G. *J. Am. Chem. Soc.* **1969**, *91*, 5440.
(4) Ban, H.; Sukegawa, K.; Tagawa, S. *Macromolecules*, **1987**, *20*, 1775, **1988**, *21*, 45.

(5) Ban, H.; Tanaka, A.; Hayashi, N.; Tagawa, S.; Tabata, Y. *Radiat. Phys. Chem*. **1989**, *34*, 587.
(6) Irie, S.; Oka, K.; Irie, M. *Maclomolecules* **1988**, *21*, 110.
(7) Irie, S.; Irie, M. *Maclomolecules* **1992**, *25*, 1766.
(8) Irie, S.; Oka, K.; Nakao, R.; Irie, M. *J. Organomet. Chem*. **1990**, *388*, 253.
(9) Ushida, K.; Kira, A.; Tagawa, S.; Yoshida, Y.; Shibata, H. *Proc. Am. Chem. Soc., Div. Polym. Mater*. **1992**, *66*, 299.
(10) Kumagai, J.; Yoshida, H.; Koizumi, H.; Ichikawa, T. *J. Phys. Chem.* **1994,** *98*, 13117.
(11) Kumagai, J.; Yoshida, H.; Ichikawa, T. *J. Phys. Chem.* **1995,** *99*, 7965.
(12) Kumagai, J.; Tachikawa, H.; Yoshida, H.; Ichikawa T. *J. Phys. Chem.* **1996,** *100*, 16777.
(13) Zhang, X.-H.; West, R. *J. Polym. Sci., Polym. Chem. Ed*. **1984**, *22*, 159.
(14) Ichikawa, T.; Yoshida, H.; Westerling, J. *J. Magn. Reson.* **1989**, *85*, 132.
(15) Ichikawa, T. *J. Chem. Phys*. **1985**, *83*, 3790.
(16) Tachikawa, H.; Ichikawa, T.; Yoshida, H. *J. Am. Chem. Soc*. **1990**, *112*, 977.
(17) Ichikawa, T.; Kevan, L.; Bowman, M. K.; Dikanov, S. A.; Tsvetkov, Yu. D. *J. Chem. Phys.* **1979**, *71*, 1167.
(18) Miller, R. D.; Michl, J. *Chem Rev*. **1989**, *89*, 1359.
(19) McCray, V. R.; Sette, F. Chen, C. T.; Lovinger, A. J.; Robin, M. B.; Stöhr, J.; Zeigler, J. M. *J. Chem Phys.* **1988**, *88*, 5925.
(20) Ichikawa, T. *J. Phys. Chem*. **1988**, *92*, 1431.
(21) Fujiki, M., *Chem. Phys. Lett*., **1992**, *198*, 177.
(22) Walsh, C.; Burland, D. M. Miller, R. D. *Chem. Phys. Lett*. **1990**, *175*, 197.
(23) Sun, Y.-P.; Miller, R. D., Sooriyakumaran, R.; Michl, J. *J. Inorg. Organomet. Polym*. **1991**, *1*, 3.
(24) Sun, Y.-P.; Wallraff, G. M.; Miller, R. D.; Michl, J. *J. Photochem. Photobiol. A: Chem.* **1991**, *62*, 333.
(25) Sun, Y.-P.; Hamada, Y.; Huang, L.−M.; Maxka, J.; Hsiao, J.−S.; West, R.; Michl, J. *J. Am. Chem. Soc.* **1992**, *114*, 1.
(26) Tilgner, A.; Trommsdorff, H. P.; Zeigler, J. M.; Hochstrasser, R. M. *J. Lumin.* **1990**, *45*, 377.
(27) Thorne, J. R. G.; Repinec, S. T.; Abrash, S. A.; Zeigler, J. M.; Hochstrasser, R. M. *Chem. Phys.* **1990**, *146*, 315.
(28) Tilgner, A.; Trommsdorff, H. P.; Zeigler, J. M.; Hochstrasser, R. M. *J. Chem. Phys.* **1992**, *96*, 781.
(29) Skinner, J. L. *J. Phys. Chem*. **1994**, *98*, 2503.